Reverse engineering field-derived vertical distribution profiles to infer larval swimming behaviors

M. K. James[a,1], J. A. Polton[b], A. R. Brereton[b], K. L. Howell[a], W. A. M. Nimmo-Smith[a], and A. M. Knights[a]

[a]School of Biological and Marine Sciences, University of Plymouth, PL4 8AA Plymouth, United Kingdom; and [b]Marine Systems Modelling Group, National Oceanography Centre, L3 5DA Liverpool, United Kingdom

Biophysical models are well-used tools for predicting the dispersal of marine larvae. Larval behavior has been shown to influence dispersal, but how to incorporate behavior effectively within dispersal models remains a challenge. Mechanisms of behavior are often derived from laboratory-based studies and therefore, may not reflect behavior in situ. Here, using state-of-the-art models, we explore the movements that larvae must undertake to achieve the vertical distribution patterns observed in nature. Results suggest that behaviors are not consistent with those described under the tidally synchronized vertical migration (TVM) hypothesis. Instead, we show (*i*) a need for swimming speed and direction to vary over the tidal cycle and (*ii*) that, in some instances, larval swimming cannot explain observed vertical patterns. We argue that current methods of behavioral parameterization are limited in their capacity to replicate in situ observations of vertical distribution, which may cause dispersal error to propagate over time, due to advective differences over depth and demonstrate an alternative to laboratory-based behavioral parameterization that encompasses the range of environmental cues that may be acting on planktic organisms.

larval behavior | vertical migration | larval swimming | reverse engineering | biophysical modeling

Larval dispersal is a primary factor shaping the distribution of marine species and influencing the structure of marine communities (1). Understanding mechanisms of dispersal is, therefore, imperative to predicting species distributions (2). Biophysical modeling—the tracking of particles assigned biological parameters ("behaviors") within ocean models—has become a ubiquitous tool for predicting propagule dispersal in the marine environment (3–5). Models have become increasingly complex to enhance "realism," yet despite these efforts, simulation outcomes often do not match the patterns observed in nature identified by genetic studies (6). As biophysical models are able to accurately predict the trajectories of abiotic particles (7), the decoupling of modeled and observed distributions is frequently attributed to poorly defined larval behavior mechanisms and a limited understanding of how to incorporate behaviors within dispersal models (6, 8).

In the context of biophysical modeling, behavior refers to applying an active swimming response, typically in the *z* dimension, to a model propagule (larvae). Planktic organisms generally swim at relatively slow speeds (millimeters to centimeters second^{-1}) in comparison with horizontal currents, which can be orders of magnitude faster (i.e., meters second^{-1}). As such, active horizontal movement, especially for the early life history stages of many marine organisms (which tend to be small), can be assumed to be passive. Swimming speeds can, however, exceed the vertical mixing velocities in the ocean (9), providing individuals with a mechanism by which they can alter their vertical position in the water column. When considered in conjunction with depth-related differences in horizontal velocity, vertical migration is argued to provide a mechanism through which weak-swimming individuals can manipulate their horizontal trajectory (10, 11). Such depth-related differences can be generated by Ekman processes, which can be

significant in both tidal (12) and open ocean environments (13), and tidally induced vertical shear (14).

Vertical swimming is often modeled in response to exogenous (i.e., external stimuli) or endogenous cues (e.g., circadian rhythm) (3, 15). This seems sensible, as laboratory studies have clearly shown that larvae can exhibit behavioral responses and directed movement in response to stimuli (16). In nature, however, organisms are likely exposed to multiple rather than single cues, which may alter their responses (17). Moreover, the scale and/or intensity of cues may be masked in nature such that behaviors observed in a laboratory are not always expressed in the field (18). As such, laboratory-observed behaviors in response to a single stimulus in a controlled environment may not be reflective of the in situ movements of larvae.

A number of field-based studies have highlighted changes in larval vertical distribution patterns that correlate with the tidal cycle: for instance, where larvae occupy surface waters during the flooding tide and remain in close proximity to the seabed during the ebbing tide or vice versa. Such tidally synchronized vertical migration (TVM) has been documented for a range of taxa (11, 19–21) across a range of larval ages (15, 22), and observations have been made in both estuarine (23, 24) and coastal (11, 25) environments. Active occupation of different depths during alternate tidal states (flood/ebb), often referred to as selective tidal stream transport (STST) (20, 26), allows organisms to exploit depth-related current differences. These observations are often interpreted as evidence of larval behavior and specifically, an energy-efficient tactic to facilitate migration over long distances or promote retention close to coastal areas. However, the mechanisms that govern tidally timed movements of marine larvae remain poorly resolved (26). Synchronization of movement with the

Significance

Estimating the dispersal of propagules in terrestrial, freshwater, and marine ecosystems has been of primary research interest for many years, yet efforts to accurately predict dispersal, especially in marine ecosystems, have remained a significant and unresolved challenge. A common approach is to use a biophysical model, but field studies and genetic tools reveal that these models can overestimate dispersal range, often attributed to inaccurate behavioral parameterization. This study reverse engineers a biophysical model in an effort to describe larval behavior. The approach demonstrated, which can be applied to any species with a larval phase, provides a method for assessing in situ larval behavior that negates the need for a mechanistic understanding of behavioral responses to cues.
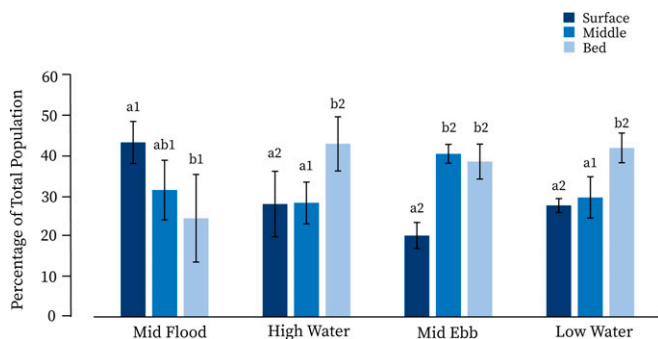
Fig. 1. Observed proportional abundance (percentage ± SD) of *Mytilus* spp. larvae within each depth zone during four tidal states (midflood, high water, midebb, and low water). Multiple comparison outcomes are shown above each bar, where different letters and numbers indicate a significant difference ($P < 0.05$) in (a and b) larval proportions between depth zones within a tidal state and (1 and 2) between tidal states within a depth zone (Tukey's honestly significant difference test).

tide suggests the presence of (*i*) cue(s) and (*ii*) behavioral decision making (27).

Research has suggested that salinity gradients may act as a cue to vertical migration (15). Salinity gradients associated with tidal state would be expected in estuaries; however, in coastal environments where tidally correlated distribution profiles have also been observed, these signals would be much weaker and thus, more difficult for larvae to detect. At coastal sites, one could assume that there would be an absence of strong tidal signals, except in velocity (28). It was recently shown that some larval fish can detect flow velocity using their lateral line, providing a navigational signal in the absence of visual or chemical cues, but it is unclear if nonfish larvae can perceive changes in the magnitude and direction of the current due to their small size and the lack of focal points in the marine environment (29). There is, however, increasing evidence to suggest that they can respond to turbulence (17), either acting as a cue for larval behavior (30, 31) or alternatively, hindering a larva's motion strategy (32) due to disorientation preventing expression of a behavioral response (33). Weinstock et al. (25) suggest that TVM patterns may be passive and caused by vertical advection resulting from the tidal flow over a sloping shelf; however, Knights et al. (11) observed a shift in abundance from the surface waters during the flood tide to deeper waters at high water (Fig. 1) that contradicts this theory. It was suggested that larvae may be responding to tidal conditions to facilitate transport, but the exact mechanism could not be resolved.

Larval behavior can be applied in biophysical models through the application of simple "rules" [e.g., TVM can be simulated by programming "larvae" to swim up during the flood and down during the ebb (or vice versa)]. This approach has been implemented in numerous studies (15, 34, 35). However, is it appropriate to apply these rules, and if so, does our current understanding of larval movement allow accurate replication of in situ patterns? Although distribution profiles in ref. 11 correlated to tidal state, the patterns observed were not analogous STST theory in which larval abundances would be expected to be greatest in the surface waters during midflood and high water to promote advection toward the coast and greatest near the bed during midebb and low water to limit offshore transport (26). Instead, larvae were most closely associated with the sea bed during both slack water periods and with the middle and bed during the ebb tide (11). Despite these observations (11), it has been heavily cited as evidence of STST and specifically used as justification for TVM in dispersal models (35). We argue that this inaccurate and will lead to erroneous predictions of dispersal. Here, using a combination of empirical data and state-of-the-art modeling, we explore the active movements

that bivalve larvae would need to undertake to create the patterns observed in nature over the course of a tidal cycle. We test a range of swimming velocities within a model environment to examine if vertical swimming could feasibly be the mechanism that facilitates the patterns observed in situ given what we know about the swimming speed of early life history stages of bivalves.

Methods

Observations of Vertical Distribution Profiles. To determine the extent of vertical migration in a coastal environment, we used data collected for a previous study (11) from two 100 × 100-m sites (site 1: 52° 19.542′ N, 6° 15.538′ W; site 2: 52° 20.036′ N, 6° 15.344′ W) within a 4-km² area with a mean depth of 24 m in the Southern Irish Sea off the coast of County Wexford, Ireland. The waters at this location are well mixed (36) with mean horizontal advection of up to 1 ms^{-1} (11) and vertical mixing at rates of up to 0.1 m² s^{-1} (Fig. 2), which can result in turbulent velocities that are orders of magnitude greater than the swimming speeds of larvae. These conditions, therefore, provide a challenging test for the effectiveness of larval behavior (e.g., swimming) to influence vertical distribution. Replicate samples ($n = 5$) were collected from three depth zones (surface, 0–8 m; midwater, 8–16 m; bottom, 16–24 m) during four consecutive tidal states (low-water slack, flood, high-water slack, ebb) over a full tidal cycle (12.1 h). Replicate sampling was undertaken in May/June and July/August to capture early- and late-stage larvae, respectively, and to encompass variation associated with differences in the tidal amplitude cycle (spring/neap). Previous analyses of the data have shown that larval vertical distribution profiles correlate to a change in the tidal state (flood, high-water slack, ebb, low-water slack) but not the tidal phase (spring/neap), ontogenetic larval stage, or sampling location. In this study, we take a numerical approach using a realistic modeled hydrodynamic environment to explore whether vertical swimming could feasibly be the mechanism that facilitates the observed changes in distribution over a tidal cycle.

The Hydrodynamic Model. A large-eddy simulation (LES) of an unstratified tidal boundary layer was used to generate a time- and depth-varying diffusivity coefficient. The purpose of the LES was to create a diffusivity matrix that represented the hydrodynamic environment at the time/location of sampling. The LES configuration was set up to be forced by time series profiles of "filtered" horizontal velocities obtained from an acoustic doppler current profiler record and solved for the turbulent "perturbation" flow (37). The LES domain was nominally 50 × 50 × 25 m, with a lateral grid size of 0.4 m and stretched vertical grid sizes of 0.07–0.17 m. This method is validated against independent measurements of turbulence dissipation. The advantage of this method over a direct three-dimensional (3D) turbulent simulation of particles comes from the fact that online Lagrangian simulations are computationally demanding. This method undertakes trajectory analysis offline using the output from the LES, reducing the computational demand
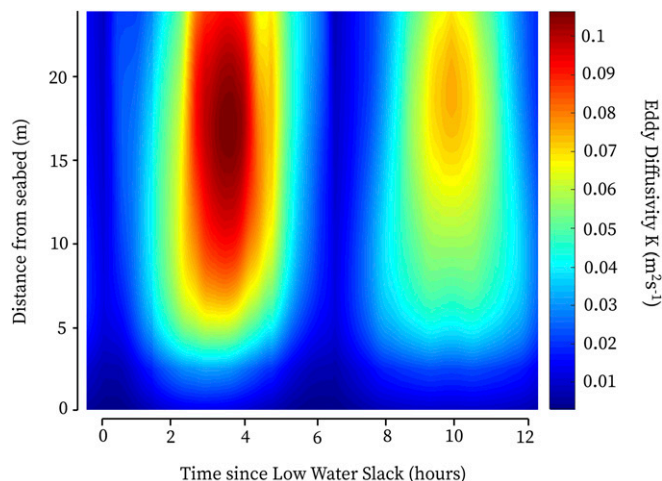

Fig. 2. Visualization of the eddy diffusivity field (K) created by the LES over a 12.1-h tidal period from low-water slack$_1$ to low-water slack$_2$ forced by time series profiles of "filtered" horizontal velocities and solved for the turbulent "perturbation" flow. Ref. 37 has full details.

ECOLOGY

of the simulation and allowing many experiments to be run to seek statistical convergence (*The Particle-Tracking Model*). In this simulation, the background tidal flow, U, was assumed to be oscillating in one direction. The direction of the flow had no influence on the resultant diffusivity coefficient. From these resolved turbulent fluctuations, an effective eddy diffusivity (Fig. 2) can be derived from the following relationship:

$$K = \frac{<u'w'>}{\frac{\partial U}{\partial z}} Pr_t,$$

where K is the eddy diffusivity (in meters^2 second^{-1}), $<u'w'>$ is a resolved Reynolds stress averaged horizontally over the domain (calculated by the LES), $\frac{\partial U}{\partial z}$ is the prescribed vertical mean (tidal) shear, and Pr_t is the turbulent Prandtl number of seawater, which is taken as one. As this statistic is not well defined when the vertical mean is near zero, a cubic spline was used to smooth K in time with 2-min intervals (38). This has no discernable effect on K away from the slack tide.

A velocity depth profile was fitted assuming a log-layer approximation with a roughness length of $z_0 = 0.001$ m, although eddy diffusivity was not sensitive to the choice of z_0. As the Irish Sea tends to be well mixed with no known hydrographic features during the spring and summer months when field samples were collected (36), it was deemed appropriate to use a constant density LES. The midpoints of the flood and ebb tide were determined from the depth-averaged current velocities when maximum positive and maximum negative flows occurred. Similarly, the slack tide midpoints were identified as the times when the associated depth-averaged current velocities were nearest to zero.

It should be noted that, as is the case with all models, the parameterized diffusivity output of the LES may not necessarily be a perfect match for what the real organisms experienced in the field. However, direct calculation of the diffusivities using an LES seems preferable to simply taking a constant value or estimating diffusivity from either a hydrostatic model or scaling arguments. Furthermore, the LES is validated to simulate realistic levels of dissipation (which represents processes at the scale of the organisms) (39). As such, it was considered an appropriate tradeoff between hydrodynamic complexity and physical accuracy while also permitting investigation into larval movement through offline particle tracking.

The Particle-Tracking Model. To test the potential of larvae to undergo vertical migration, a 1D Lagrangian particle-tracking algorithm was built in MATLAB (version 2017b) to follow the vertical trajectories of virtual larvae within the filtered eddy diffusivity flow field as generated by the LES. The 1D definition of the particle tracker is due to the exclusion of horizontal movement within the simulation (i.e., eddy diffusivity can only move particles upward or downward). Preliminary tests using 100, 10,000, and 100,000 seed particles indicated convergence of the relative vertical distribution profiles. As such, it was deemed appropriate to use 100 particles in each simulation to minimize computational effort without influencing results.

The hydrodynamic environment was prescribed using the horizontally averaged output of the LES, K, which was coupled with a particle movement component implemented using a random walk approach (as described in ref. 40) and larval active swimming (ω) behavior (described in detail below). The model timestep, δt, was set at 60 s. This was deemed sufficiently small enough so that the diffusivity profile was locally well approximated by the first-order Taylor expansion. Particle movement was calculated for δt by

$$z_{n+1} = z_n + K'(z_n)\delta t + R\left[\frac{2K(z_n + \frac{1}{2}K'(z_n)\delta t)\delta t}{r}\right]^{0.5} + \omega_n \delta t,$$

where z_n is the depth of a particle at the nth timestep, K' is the diffusivity gradient at the particle location ($\delta K/\delta z$), R is a random number from a continuous distribution between 1 and −1 (with variance $r = 0.33$), and ω_n is the vertical swimming velocity of a particle at timestep n.

A Mersenne–Twister algorithm was applied to the random number generator to ensure that values of R were sufficiently random. The inclusion of the deterministic component $K'(z_n)\delta t$ ensures that particles are always advected in the direction of higher diffusivity, thus preventing artificial accumulation in low-diffusion areas. It was assumed that the rate of larval diffusivity was equal to the rate of eddy diffusivity calculated by the LES. This was considered appropriate, as larval transport by eddies is not affected by inertial and crossing trajectories effects due to their small size (40).

Larval vertical movement was explored from each tidal state to the next consecutive state (flood to high water, high water to ebb, ebb to low water, low water to flood) using a "mixed model" approach. Before each simulation, the model water column was seeded with particles in a probabilistic

vertical distribution profile based on the observed vertical distribution for the defined starting tidal state. To achieve this, the model particles ($n = 100$) were distributed so that the percentage of particles in each bin matched the percentage of the total population of larvae observed in the field for that bin/tidal state. Additionally, particles were randomly assigned depths within each depth bin using a random number generator. Particles were then assigned "behavioral rules," which are explained in additional detail below.

Parameterizing Swimming Behavior. To assess the influence of larval swimming on vertical distribution profiles, multiple simulations were run using a range of swimming velocities ($n = 2,525$). Although bivalve larvae have been observed to swim in a helical pattern (41), swimming in the model was confined to one dimension, and as such, swimming velocities represent the absolute swimming velocity (the vertical distance traveled by an organism) rather than the linear velocity (the velocity of a larva along its swimming path). Swimming velocities explored ranged from −2.5 to 5 mm s^{-1}, justified by an in-depth literature review (30, 42). Particles were considered neutrally buoyant (i.e., downward movement was an active response) and swam constantly at the swimming velocity given by the model parameters.

Each simulation ran from the midpoint of the defined starting tidal state to the midpoint of the next consecutive state. Simulation duration was variable: 174 model minutes between low water and midflood, 176 min between midflood and high water, 198 min between high water and midebb, and 182 min between midebb and low water. Variation matched that at the survey location, where local bathymetry can act to distort the pattern of the tide, generating tidal asymmetry (43). Furthermore, around the British Isles, the M_2 and M_4 tides can combine to give differences in the flood and ebb tidal streams (44). Tidal asymmetry has been demonstrated in the Irish Sea (45) and was observed by Knights et al. (11) at the study site. Such patterns were replicated by the LES.

After each simulation, the proportional abundance of particles within each depth bin was calculated (where the proportion is the number of particles in each bin divided by the total number of seeded model particles) and compared with the observed proportional abundance of particles for the end tidal state of the model run.

Larval Vertical Velocity as a Predictor of in Situ Distribution Profiles. A bootstrap approach was used to assess the error between the modeled and observed profiles for each tested vertical velocity at each tidal state given the variation in the sampled (modeled and observed) populations. We generated 100 estimates of the observed distribution profile using the mean and SD of the observed proportional abundances in each depth bin ($n = 5$). We then used the same method to bootstrap 100 distribution profiles for each tested swimming velocity using the modeled proportional abundances in each depth bin as the sample data ($n = 25$). Pairwise comparisons were used to determine the sum of squares of the proportional difference between the simulated and observed profiles for each depth bin, and the overall difference between the observed and simulated profiles was demonstrated by the total of the sum of squares of the difference for all three bins (SS$_{total}$). The mean square error (MSE) and 95% confidence intervals were calculated for each tested velocity. SS$_{total}$ ($n = 7,600$ for each tidal period: 100 pairwise comparisons × 76 tested swimming velocities) and MSE ($n = 76$) were plotted against swimming velocity. Best-fitting curves were constructed in R using ANOVA to justify the order of the polynomial. The equation of each curve was then solved for the smallest value of y to determine the swimming velocity where the likelihood of difference between the simulated and observed profiles was lowest and as such, the quality of that velocity as a predictor of in situ distribution patterns was greatest.

Assessing Model Compatibility. Two-way ANOVA and planned F-test comparisons were used to compare proportions of larvae recorded from in situ observations ($n = 5$) and proportions of virtual larvae from model simulations ($n = 5$) (46). For each tested velocity, the number of simulation runs was fixed to match the number of replicates observed. As proportional distribution data were in percentages, data were transformed by the angular (arcsine of square root) transformation before statistical analysis to satisfy the assumptions of the ANOVA. The simulation was replicated five times for each scenario to generate variance estimates around the mean diffusivity based on the random walk. Stouffer's transformed z method (47) was used to combine the P values of the interaction term of the five independently run tests to provide a quantifiable continuous measure of compatibility between the observed data and the model outcome—model predictive capability (MPC)—ranging from zero (complete incompatibility) to one (perfect compatibility) (48). In addition to the continuous measure of compatibility, the combined P value was used at the significance level of 0.01 (Bonferroni

Results

The success of the model at predicting the distribution profiles observed in nature was highly variable and dependent on tidal period modeled and swimming velocity assigned to the particles as demonstrated by the MPC (Fig. 3, bars). When particles were passive, the modeled distribution profile was significantly different from the observed profile for all tidal states (Stouffer's $P < 0.01$). On the flood tide, modeled distribution profiles did not significantly differ from those observed in nature when particles were assigned swimming velocities ranging from 0.8 to 3.3 mm s^{-1} (Stouffer's $P > 0.01$), and maximum MPC (MPC$_{max}$) was achieved at 2.2 mm s^{-1} (Stouffer's $P = 0.997$) (Fig. 3A). MPC$_{max}$ at high water was achieved when particles were assigned a swimming velocity of −0.8 mm s^{-1} (Stouffer's $P = 0.883$), and velocities between −0.4 and −1.5 mm s^{-1} produced profiles that did not significantly differ from the observations (Stouffer's $P > 0.01$), with the exception of −1.4 mm s^{-1} (Stouffer's $P < 0.01$) (Fig. 3B). The model predicted distributions were not significantly different from those observed at low water when particles were assigned swimming velocities of −0.7, −0.8, and −1 mm s^{-1} tide (Stouffer's $P > 0.01$), with MPC$_{max}$ at −0.7 and −0.8 mm s^{-1} tide (Stouffer's $P = 0.23$ for both) (Fig. 3D). Combined P values suggest significant differences between the modeled and observed distribution profiles on the ebb tide for all tested swimming velocities (Fig. 3C), and therefore, a value for MPC$_{max}$ on the ebb tide could not be determined.

Minimum SS$_{total}$, as predicted by the fitted curves, correlated well to MPC$_{max}$ (Fig. 3), with the lowest values predicted within 2 mm s^{-1} of the swimming velocities related to MPC$_{max}$ for the flood tide (Velocity$_{Min.SStotal}$ = 2.4 mm s^{-1}; MPC$_{max}$ = 2.2 mm s^{-1}) (Fig. 3A), high water (Velocity$_{Min.SStotal}$ = −1 mm s^{-1}; MPC$_{max}$ = −0.8 mm s^{-1}) (Fig. 3B), and low water (Velocity$_{Min.SStotal}$ = −0.8 mm s^{-1}; MPC$_{max}$ = −0.7/−0.8 mm s^{-1}) (Fig. 3D). The velocity at which the lowest SS$_{total}$ was predicted on the ebb tide was −1.1 mm s^{-1} (Fig. 3C).

Discussion

Behavior is often included in biophysical models using relatively simple rules based on laboratory-based observations of larval responses to cues (15, 35). Here, we argue that this approach may not be appropriate. Our results suggest that current methods of behavioral parameterization used in biophysical modeling studies are limited in their capacity to "match" in situ observations of vertical distribution profiles. Using a bootstrap approach, we identified the swimming velocities that best reduced the likelihood of difference between observed distributions and those predicted by the model, even in instances where the MPC was low (i.e., the ebb tide).

We simulated change in the vertical distribution of virtual larvae by assigning "behaviors" to particles within a high-resolution tidal boundary-layer Lagrangian model. To our knowledge, there is no study that has attempted to reverse engineer model simulations to determine larval behavioral parameters in this way. In addition to showing that the likelihood of difference between model and nature is reduced when particles are assigned some sort of active movement compared with passive particles, our results indicate when larvae change their swimming "behavior" in response to changes in tidal state. We showed that a shift from positive (upward) to negative (downward) movement around the midflood point of the circatidal cycle was necessary for larvae to achieve the distribution patterns observed in nature (11). This is counter to the STST hypothesis, which argues that organisms swim upward for the duration of one tidal state and downward during the opposing state (49), and it contradicts the theory of Weinstock et al. (25) of passive vertical advective movement by tidal straining, as this mechanism would result in the direction of vertical movement being consistent during the flooding tide. Consequently, the implementation of TVM in a dispersal model using this "rule" (35) may be ineffective at generating vertical profiles that accurately represent nature. Even over relatively short time periods, such as the 3-h period between midflood and high water, inaccurate vertical distributions in biophysical models will influence dispersal estimates, and such errors will accumulate and propagate over time (consider species with long planktic larval durations). This effect was recently hypothesized by Firth et al. (50). Looking forward, future research should explore how the results of this study propagate through the larval dispersal estimated by a biophysical model and how behavioral parameters derived from the reverse engineering of in situ vertical distribution profiles influence both dispersal and connectivity predictions compared with estimates
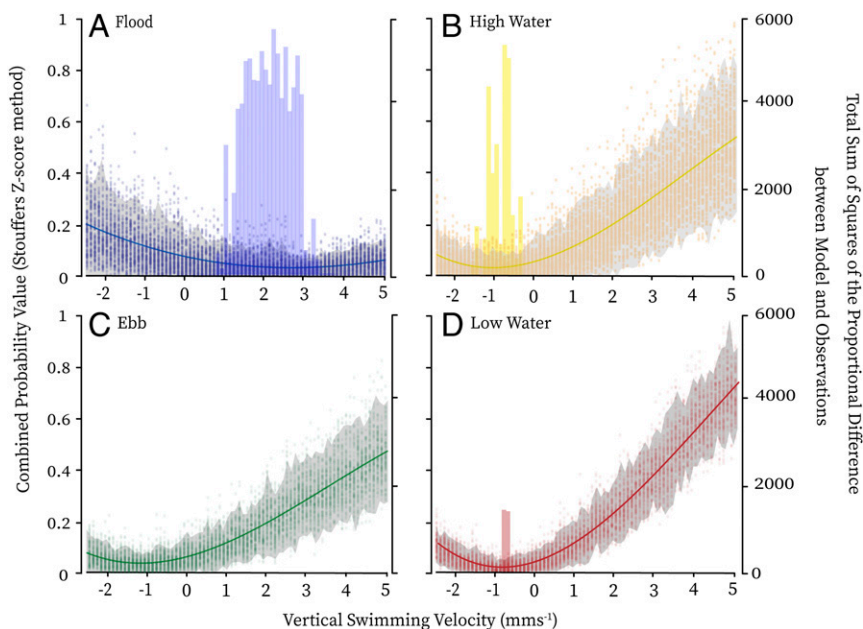

Fig. 3. Compatibility of the model with predicting the distribution profiles observed in nature during (*A*) the flood tide, (*B*) high-water slack, (*C*) the ebb tide, and (*D*) low-water slack after an ~3-h simulation period and the quality of vertical swimming velocity as an estimator of observed profiles. Vertical swimming velocity (millimeters second^{-1}) is shown against MPC (Stouffer's combined *P* value; colored bars; left axis) and total sum of squares of the difference between 100 pairwise comparisons of modeled and observed distribution profiles generated using a bootstrap approach (right axis). Data points indicate individual pairwise comparisons (*n* = 7,600), and gray bands demonstrate 95% confidence intervals. MSE is represented by colored lines. Curves of best fit are calculated using third-order polynomials. (*A*) Flood: $y = -1.18x^3 + 43x^2 - 193.16x + 448.48$; $r^2 = 0.39$ (SS$_{total}$); $r^2 = 0.97$ (MSE). (*B*) High water: $y = -9.95x^3 + 122.25x^2 + 276.62x + 363.19$; $r^2 = 0.75$ (SS$_{total}$); $r^2 = 0.99$ (MSE). (*C*) Ebb: $y = -9.05x^3 + 91.61x^2 + 252.34x + 379.60$; $r^2 = 0.82$ (SS$_{total}$); $r^2 = 0.99$ (MSE). (*D*) Low water: $y = -13.49x^3 + 170.38x^2 + 335.67x + 251.78$; $r^2 = 0.93$ (SS$_{total}$); $r^2 = 0.99$ (MSE).

ECOLOGY

made using alternative approaches to vertical distribution [i.e., "rule-based" behaviors (35)] and/or probabilistic larval vertical distribution profiles (51).

All velocities resulting in the smallest error between model and observations fell between the boundaries of larval swimming reported in the literature, suggesting that swimming is an important mechanism. Reported swimming speeds and sinking velocity estimates are typically highly variable both within and across taxa, although they are typically in the range of 1–10 mm s^{-1} and rarely exceed 20 mm s^{-1} (4.2 cm s^{-1} in *Cancer magister* megalopa) (52). Our study showed that, for our data, upward swimming must be 2.5× faster than downward swimming to best match the observed profiles. This demonstrates the need for swimming speed to be a variable parameter in dispersal modeling studies and highlights that the speeds of upward and downward movements are not always consistent; however, we acknowledge that any difference in optimum swimming speed among tidal states will be most marked in slower swimming species, such as bivalves, and effects will likely be less pronounced for stronger swimmers (53).

The model-generated distribution profiles on the ebb tide were significantly different from those observed for all tested velocities, leading to low model compatibility (high water to midebb; midebb to low water). This is in marked contrast to the flood tide, where compatibility was high. Our approach was able to identify the optimum vertical velocities that give the "best fit" to the observed patterns when larval behavior is parameterized by constant swimming in one direction; however, the low compatibility between the modeled data and observed profiles suggests that we do not fully understand the behavioral responses of the larvae and their relationship with the physical characteristics of the ocean during this particular tidal state. For instance, it is possible that spatially and/or temporally inconsistent behavioral responses in situ may cause larval swimming to differ among depths over even shorter timescales. One possible solution to this problem might be to use higher spatiotemporal resolution in situ sampling coupled with a short model internal timestep in an effort to improve model compatibility. This process alone may provide further insights into the relationship between manifestation of larval behaviors in response to their environment while simultaneously supporting improved model compatibility and better characterization of larval behavior within model frameworks.

Due to the sampling regime of the original study, our model was only able to reverse engineer optimum swimming speeds during daylight hours. Diel vertical migration (DVM) occurs when organisms synchronize their vertical movement to the day/night cycle. Such behavior, thought to be a predation avoidance response (54), has been documented for a number of taxa (55–57). Whether bivalve larvae exhibit DVM remains unclear; there is conflicting evidence in the literature (57, 58), and differences may well be location specific. Future research would benefit from sampling programs that encompass the 24-h diel cycle to encapsulate potential variation in the vertical distribution of larvae within the study domain due to the day/night cycle.

The model system of this study assumes a well-mixed open coastal environment with a flat bathymetry and laterally homogenous spatially averaged velocities. Given this and the fact that the LES model could be directly forced by observed velocities suggest that the LES data broadly described the hydrodynamic conditions that the larvae would experience throughout the study domain. It must be noted, however, that, in environments with high spatial heterogeneity (for example, over sloping bathymetry or across lateral or vertical frontal systems), differential vertical mixing may influence larval ability to regulate depth as expected. Stratification of the water column has been shown to alter the vertical migration of marine organisms (57, 59) by acting as a barrier to vertical movement (60). Should our approach be undertaken to infer larval swimming in a more heterogeneous environment, such as an estuary, the underlying hydrodynamic model should be designed as to adequately represent realistic conditions.

The cues that govern larval swimming responses in situ remain unclear and were beyond the scope of this study. It has been previously suggested that some larvae may respond to a hierarchy of cues; indeed, many have the sensory ability to do so (16, 28). Hierarchical responses to stimuli have been shown to influence the vertical migration of a range of taxa, including the larvae of sponges (18) and fish (61), and therefore, it is possible that a similar response exists in other organisms: for example, bivalves. If cues do influence the vertical migration of larvae in a hierarchical manner, their order of importance to the organism must be determined if behaviors are to be parameterized using a rule-based approach in dispersal models so that behaviors accurately depict responses in nature. This order may change over space and time and in relation to other cues, and therefore, rule-based models must account for this. Failure to do so could greatly contribute to model error.

With this in mind, accurately parameterizing larval behavior using a rule-based approach is clearly a complex endeavor that requires an in-depth understanding of a multitude of potential drivers of larval movement and knowledge of how these drivers influence both larvae and each other. Using field-derived vertical distribution data to set the goal posts, our approach allows larval behavior to be based on real-life changes in the vertical distribution patterns of larvae. By focusing on the active movements particles would be required to undertake within the model domain to achieve a distribution profile that is the least different from that observed in nature, we effectively bypass the need for a complex understanding of the mechanisms of planktic swimming and larval responses to behavioral stimuli, instead, we focus on the end goal: achieving a modeled distribution profile that accurately replicates nature.

Dispersal is a key mechanism that shapes the distribution of marine species, and thus, an understanding of how and why species disperse is imperative to the success of marine conservation agendas, fisheries management efforts, and attempts to minimize the risk of invasive species spread (2, 62, 63). Biophysical modeling provides a cost-effective tool to estimate dispersal in the marine environment; however, inaccuracies within these models can misguide those using them, and consequently, decisions made off the back of inaccurate model estimations may be ineffective (64). This study demonstrates that active movement changes over the course of the tidal cycle at temporal scales typically not modeled. Our approach has reverse engineered model simulations to identify the larval swimming speeds and directions that generate the smallest error between modeled and observed distribution patterns. These estimates are not perfect, but as error is reduced compared with the passive model when particles are given active movement, we can conclude that larval swimming is an important mechanism in accurate depictions of vertical distribution. This approach will allow future research to determine the best-fitting behaviors of a range of taxa, where in situ vertical distribution data are/can be made available.

This study highlights that, over a period as short as 12 h, differences in behavior (i.e., speed/direction) required to replicate observed vertical distribution profiles are great. Our results indicate that current "rule-based" approaches to behavioral parameterization [for example, assigning a constant swimming speed to particles and/or assuming vertical direction with respect to tidal direction (35)] may lead to significant over- or underestimates of dispersal. For larvae swimming outside optimum speeds, modeled predictions of dispersal will become increasingly divergent over time in terms of match to in situ observations due to depth-related differences in current velocity, especially for species with planktonic larval durations longer than 1 d. This study offers an alternative

method of behavioral parameterization where behavior is inferred from the field rather than the laboratory, which will aid in minimizing the error associated with inaccurate vertical distribution profiles in biophysical models.

1. R. K. Cowen, S. Sponaugle, Larval dispersal and marine population connectivity. *Annu. Rev. Mar. Sci.* **1**, 443–466 (2009).
2. L. A. Levin, Recent progress in understanding larval dispersal: New directions and digressions. *Integr. Comp. Biol.* **46**, 282–297 (2006).
3. N. S. Banas, P. S. McDonald, D. A. Armstrong, Green crab larval retention in Willapa Bay, Washington: An intensive Lagrangian modeling approach. *Estuaries Coasts* **32**, 893–905 (2009).
4. A. Nicolle, F. Dumas, A. Foveau, E. Foucher, E. Thiebaut, Modelling larval dispersal of the king scallop (Pecten maximus) in the English channel: Examples from the bay of Saint-Brieuc & the bay of Seine. *Ocean Dyn.* **63**, 661–678 (2013).
5. R. E. Ross, A. W. Nimmo-Smith, K. L. Howell, Towards 'ecological coherence': Assessing larval dispersal within a network of existing marine protected areas. *Deep Sea Res. Part I Oceanogr. Res. Pap.* **126**, 128–138 (2017).
6. D. J. Marshall, K. Monro, M. Bode, M. J. Keough, S. Swearer, Phenotype-environment mismatches reduce connectivity in the sea. *Ecol. Lett.* **13**, 128–140 (2010).
7. R. L. Soulsby, C. T. Mead, B. R. Wild, "A model for simulating the dispersal tracks of sand grains in coastal areas–"SandTrack" in *Coastal and Shelf Sediment Transport*, P. S. Balson, M. B. Collins, Eds. (Geological Society Special Publications, 2007), Book 274, pp. 65–72.
8. A. Metaxas, M. Saunders, Quantifying the "bio-" components in biophysical models of larval transport in marine benthic invertebrates: Advances and pitfalls. *Biol. Bull.* **216**, 257–272 (2009).
9. S. Thorpe, *The Turbulent Ocean* (Cambridge University Press, Cambridge, 2005).
10. C. Porch, A theoretical comparison of the contributions of random swimming & turbulence to absolute dispersal in the sea. *Bull. Mar. Sci.* **62**, 31–44 (1998).
11. A. M. Knights, T. P. Crowe, G. Burnell, Mechanisms of larval transport: Vertical distribution of bivalve larvae varies with tidal conditions. *Mar. Ecol. Prog. Ser.* **326**, 167–174 (2006).
12. J. A. Polton, M. R. Palmer, M. J. Howarth, The vertical structure of time-mean estuarine circulation in a shallow, rotating, semi-enclosed coastal bay: A Liverpool Bay case study with application for monitoring. *Cont. Shelf Res.* **59**, 115–126 (2013).
13. J. A. Polton, Y.-D. Lenn, S. Elipot, T. K. Chereskin, J. Sprintall, Can Drake Passage observations match Ekman's classic theory. *J. Phys. Oceanogr.* **48**, 1733–1740 (2013).
14. R. J. Uncles, J. A. Stephens, The structure of vertical current profiles in a macrotidal partly-mixed estuary. *Estuaries* **13**, 349–361 (1990).
15. E. W. North et al., Vertical swimming behavior influences the dispersal of simulated oyster larvae in a coupled particle-tracking & hydrodynamic model of Chesamide Bay. *Mar. Ecol. Prog. Ser.* **359**, 99–115 (2008).
16. M. J. Kingsford et al., Sensory environments, larval abilities & local self-recruitment. *Bull. Mar. Sci.* **70**, 309–340 (2002).
17. J. Welch, R. Forward, Flood tide transport of blue crab, Callinectes sapidus, postlarvae: Behavioral responses to salinity & turbulence. *Mar. Biol.* **139**, 911–918 (2001).
18. P. Ettinger-Epstein, S. Whalan, C. N. Battershill, R. de Nys, A hierarchy of settlement cues influences larval behaviour in a coral reef sponge. *Mar. Ecol. Prog. Ser.* **365**, 103–113 (2008).
19. W. J. Kimmerer, J. R. Burau, W. A. Bennett, Tidally oriented vertical migration & position maintenance of zooplankton in a temperate estuary. *Limnol. Oceanogr.* **43**, 1697–1709 (1998).
20. M. M. Criales, M. B. Robblee, J. A. Browder, H. Cardenas, T. L. Jackson, Field observations on selective tidal-stream transport for postlarval & Juvenile Pink Shrimp in Florida Bay. *J. Crustac. Biol.* **31**, 26–33 (2011).
21. H. Ueda, M. Kuwatani, K. W. Suzuki, Tidal vertical migration of two estuarine copepods: Naupliar migration & position-dependent migration. *J. Plankton Res.* **32**, 1557–1572 (2010).
22. R. A. Lutz, M. J. Kennish, "Ecology and morphology of larval and early larval postlarval mussels" in *The Mussel Mytilus: Ecology, Physiology, Genetics and Culture*, E. M. Gosling, Ed. (Developments in Aquaculture and Fisheries Science, no. 25, Elsevier Science Publishers, Amsterdam, 1992), pp. 53–85.
23. H. B. Kunze, S. G. Morgan, M. L. Kamazima, Field test of the behavioural regulation of larval transport. *Mar. Ecol. Prog. Ser.* **487**, 71–87 (2013).
24. L. G. Peteiro, A. L. Shanks, Up and down in the bay: Retentive strategies of Olympia oyster larvae in a shallow estuary. *Mar. Ecol. Prog. Ser.* **530**, 103–117 (2015).
25. J. B. Weinstock, S. L. Morello, L. M. Conlon, H. Xue, P. O. Yund, Tidal shifts in the vertical distribution of bivalve larvae: Vertical advection vs. active behaviour. *Limnol. Oceanogr.* **63**, 2681–2694 (2018).
26. R. B. Forward, R. A. Tankersley, Selective tidal-stream transport of marine animals. *Oceanogr. Mar. Biol. Annu. Rev.* **39**, 305–353 (2001).
27. R. N. Gibson, Go with the flow: Tidal migration in marine animals. *Hydrobiol.* **503**, 153–161 (2003).
28. P. Oteiza, I. Odstrcil, G. Lauder, R. Portugues, F. Engert, A novel mechanism for mechanosensory-based rheotaxis in larval zebrafish. *Nature* **547**, 445–448 (2017).
29. M. A. McManus, C. B. Woodson, Plankton distribution and ocean dispersal. *J. Exp. Biol.* **215**, 1008–1016 (2012).
30. H. L. Fuchs, C. DiBacco, Mussel larval responses to turbulence are unaltered by larval age or light conditions. *Limnol. Oceanogr. Fluids Environ.* **1**, 120–134 (2011).
31. H. L. Fuchs, E. J. Hunter, E. L. Schmitt, R. A. Guazzo, Active downward propulsion by oyster larvae in turbulence. *J. Exp. Biol.* **216**, 1458–1469 (2013).
32. F. G. Michalec, S. Souissi, M. Holzner, Turbulence triggers vigorous swimming but hinders motion strategy in planktonic copepods. *J. R. Soc. Interface* **12**, 150–158 (2015).
33. C. J. Bradley, J. R. Strickler, E. J. Buskey, P. H. Lenz, Swimming and escape behavior in two species of calanoid copepods from nauplius to adult. *J. Plankton Res.* **35**, 49–65 (2013).
34. C. B. Paris, J. B. Helgers, E. van Sebille, A. Srinivasan, Connectivity modeling system: A probabilistic modeling tool for the multi-scale tracking of biotic & abiotic variability in the ocean. *Environ. Model. Softw.* **42**, 47–54 (2013).
35. P. E. Robins, S. P. Neill, L. Giménez, A numerical study of marine larval dispersal in the presence of an axial convergent front. *Estuar. Coast. Shelf Sci.* **100**, 172–185 (2012).
36. J. Brown et al., Observations of the physical structure & seasonal jet-like circulation of the Celtic Sea & St. George's channel of the Irish Sea. *Cont. Shelf Res.* **23**, 533–561 (2003).
37. A. R. Brereton, A. Tejada-Martinez, M. R. Palmer, J. A. Polton, The perturbation method–A novel large-eddy simulation technique to model realistic turbulence: Application to tidal flow. *Ocean Model.* **135**, 31–39 (2019).
38. C. de Boor, *A Practical Guide to Splines* (Springer-Verlag, New York, 1978).
39. A. Metaxas, Behaviour in flow: Perspectives on the distribution & dispersion of meroplanktonic larvae in the water column. *Can. J. Fish. Aquat. Sci.* **58**, 86–98 (2001).
40. O. N. Ross, J. Sharples, Recipe for 1-D Lagrangian particle tracking models in space-varying diffusivity. *Limnol. Oceanogr. Methods* **2**, 289–302 (2004).
41. P. R. Jonsson, C. André, M. Lindegarth, Swimming behaviour of marine bivalve larvae in a flume boundary-layer flow: Evidence for near-bottom confinement. *Mar. Ecol. Prog. Ser.* **79**, 67–76 (1991).
42. M. Sprung, Physiological energetics of mussel larvae (Mytiius edulis). III. Respiration. *Mar. Ecol. Prog. Ser.* **18**, 171–178 (1984).
43. J. Dronkers, Tidal asymmetry & estuarine morphology. *Neth. J. Sea Res.* **20**, 117–131 (1986).
44. R. D. Pingree, D. K. Griffiths, S& transport paths around the British Isles resulting from M2 & M4 tidal interactions. *J. Mar. Biol. Assoc. U. K.* **59**, 497–513 (1979).
45. R. D. Moore, J. Wolf, A. J. Souza, S. S. Flint, Morphological evolution of the Dee Estuary, Eastern Irish sea, UK: A tidal asymmetry approach. *Geomorphology* **103**, 588–596 (2009).
46. R. Sokal, F. Rohlf, *Biometry* (W. H. Freeman & Co., New York, 1995).
47. S. A. Stouffer, E. A. Suchman, L. C. DeVinney, S. A. Star, R. M. Williams Jr, *The American Soldier, Vol. 1: Adjustment During Army Life* (Princeton University Press, Princeton, 1949).
48. S. Greenland et al., Statistical tests, P values, confidence intervals, and power: A guide to misinterpretations. *Eur. J. Epidemiol.* **31**, 337–350 (2016).
49. C. V. Civelek, R. M. Daigle, A. Metaxas, Effects of temperature on larval swimming patterns regulate vertical distribution relative to thermoclines in Asterias rubens. *J. Exp. Mar. Biol. Ecol.* **445**, 1–12 (2013).
50. L. B. Firth et al., Ocean sprawl: Challenges and opportunities for biodiversity management in a changing world. *Oceanogr. Mar. Biol. Annu. Rev.* **54**, 193–269 (2016).
51. C. B. Paris, L. M. Cherubin, R. K. Cowen, Surfing, spinning or diving: Effects on population connectivity. *Mar. Ecol. Prog. Ser.* **347**, 285–300 (2007).
52. F.-S. Chia, J. Buckland-Nicks, C. M. Young, Locomotion of marine invertebrate larvae: A review. *Can. J. Zool.* **62**, 1205–1222 (1984).
53. M. E. Huntley, M. Zhou, Influence of animals on turbulence in the sea. *Mar. Ecol. Prog. Ser.* **273**, 65–79 (2004).
54. W. Lampert, Ultimate causes of diel vertical migration of zooplankton: New evidence for the predator-avoidance hypothesis. *Ergebnisse Limnol.* **39**, 79–88 (1993).
55. M. R. Romero et al., Larval diel vertical migration of the marine gastropod Kelletia kelletii (Forbes, 1850). *J. Mar. Biol.* **2012**, 1–9 (2012).
56. J. K. Breckenridge, S. M. Bollens, Vertical distribution and migration of decapod larvae in relation to light and tides in Willapa Bay, Washington. *Estuaries Coasts* **34**, 1255–1261 (2011).
57. D. Raby, Y. Lagadeuc, J. J. Dodson, M. Mingelbier, Relationship between feeding and vertical distribution of bivalve larvae in stratified and mixed waters. *Mar. Ecol. Prog. Ser.* **103**, 275–284 (1994).
58. J. Bonicelli et al., Diel vertical migration and cross-shore distribution of barnacle and bivalve larvae in the central Chile inner-shelf. *J. Exp. Mar. Biol. Ecol.* **485**, 35–46 (2016).
59. L. A. Lougee, S. M. Bollens, S. R. Avent, The effects of haloclines on the vertical distribution and migration of zooplankton. *J. Exp. Mar. Biol. Ecol.* **278**, 111–134 (2002).
60. R. M. Daigle, A. Metaxas, Vertical distribution of marine invertebrate larvae in response to thermal stratification in the laboratory. *J. Exp. Mar. Biol. Ecol.* **409**, 89–98 (2011).
61. M. A. Teodosio, C. B. Paris, E. Wolankski, P. Morias, Biophysical processes leading to the ingress of temperate fish larvae into estuarine nursery areas: A review. *Estuar. Coast. Shelf Sci.* **183**, 187–202 (2016).
62. L. Botsford, F. Micheli, A. Hastings, Principles for the design of marine reserves. *Ecol. Appl.* **13**, S25–S31 (2003).
63. S. Palumbi, Population genetics, demographic connectivity & the design of marine reserves. *Ecol. Appl.* **13**, S146–S158 (2003).
64. L. W. Botsford et al., Connectivity and resilience of coral reef metapopulations in marine protected areas: Matching empirical efforts to predictive needs. *Coral Reefs* **28**, 327–337 (2009).

ECOLOGY